

Synthesis and Properties of the Heterospin ($S_1 = S_2 = 1/2$) Radical-Ion Salt Bis(mesitylene)molybdenum(I) [1,2,5]Thiadiazolo[3,4-*c*][1,2,5]thiadiazolidyl

Nikolay A. Pushkarevsky,^{†,‡} Nikolay A. Semenov,[‡] Alexey A. Dmitriev,^{§,#} Natalia V. Kuratieva,^{†,‡} Artem S. Bogomyakov,^{||} Irina G. Irtegovva,^{‡,‡} Nadezhda V. Vasileva,[‡] Bela E. Bode,[∇] Nina P. Gritsan,^{*,§,#} Lidia S. Konstantinova,[○] J. Derek Woollins,[∇] Oleg A. Rakitin,[○] Sergey N. Konchenko,^{†,‡} Victor I. Ovcharenko,^{||} and Andrey V. Zibarev^{*,‡,#,◆}

[†]Institute of Inorganic Chemistry, [‡]Institute of Organic Chemistry, [§]Institute of Chemical Kinetics and Combustion, and ^{||}International Tomography Center, Siberian Branch of the Russian Academy of Sciences, 630090 Novosibirsk, Russia

[‡]Department of Natural Sciences and [#]Department of Physics, Novosibirsk State University, 630090 Novosibirsk, Russia

[∇]EaStCHEM School of Chemistry and Centre of Magnetic Resonance, University of St. Andrews, St. Andrews, Fife KY16 9ST, United Kingdom

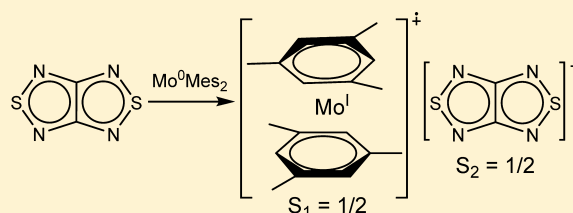
[○]Institute of Organic Chemistry, Russian Academy of Sciences, 119991 Moscow, Russia

[◆]Department of Chemistry, Tomsk State University, 634050 Tomsk, Russia

Supporting Information

ABSTRACT: Low-temperature interaction of [1,2,5]thiadiazolo[3,4-*c*][1,2,5]thiadiazole (**1**) with MoMes₂ (Mes = mesitylene/1,3,5-trimethylbenzene) in tetrahydrofuran gave the heterospin ($S_1 = S_2 = 1/2$) radical-ion salt [MoMes₂]⁺[**1**]⁻ (**2**) whose structure was confirmed by single-crystal X-ray diffraction (XRD). The structure revealed alternating layers of the cations and anions with the Mes ligands perpendicular, and the anions tilted by 45°, to the layer plane. At 300 K the effective magnetic moment of **2** is equal to 2.40 μ_B

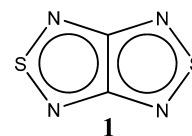
(theoretically expected 2.45 μ_B) and monotonically decreases with lowering of the temperature. In the temperature range 2–300 K, the molar magnetic susceptibility of **2** is well-described by the Curie–Weiss law with parameters *C* and θ equal to 0.78 cm³ K mol⁻¹ and –31.2 K, respectively. Overall, the magnetic behavior of **2** is similar to that of [CrTol₂]⁺[**1**]⁻ and [CrCp*₂]⁺[**1**]⁻, i.e., changing the cation [MAr₂]⁺ 3d atom *M* = Cr (*Z* = 24) with weak spin–orbit coupling (SOC) to a 4d atom *M* = Mo (*Z* = 42) with stronger SOC does not affect macroscopic magnetic properties of the salts. For the XRD structure of salt **2**, parameters of the Heisenberg spin-Hamiltonian were calculated using the broken-symmetry DFT and CASSCF approaches, and the complex 3D magnetic structure with both the ferromagnetic (FM) and antiferromagnetic (AF) exchange interactions was revealed with the latter as dominating. Salt **2** is thermally unstable and slowly loses the Mes ligands upon storage at ambient temperature. Under the same reaction conditions, interaction of **1** with MoTol₂ (Tol = toluene) proceeded with partial loss of the Tol ligands to afford diamagnetic product.



INTRODUCTION

In the design and synthesis of new molecule-based magnetic materials, the metal-radical approach dealing with coordination compounds of paramagnetic metal cations and organic radical ligands, both neutral and negatively charged (i.e., radical anions, RAs), can be very useful.^{1–3} Recently, it was shown that thiazyl RAs, derivatives of 1,2,5-thiadiazole and 1,2,3-dithiazole ring systems, can be used in preparing magnetically active RA salts.^{4,5} An especially effective approach is reduction of heterocycles such as [1,2,5]thiadiazolo[3,4-*c*][1,2,5]thiadiazole (**1**, Chart 1) to their RAs with organometallics MR₂ (*M* = Co, Cr, *R* = Cp, Cp*; *M* = Cr, *R* = Ar) allowing the synthesis of both homo- and heterospin RA salts.^{6,7} The resultant salts have complex magnetic structures dominated by antiferromagnetic (AF) exchange interactions associated within the McConnell I

Chart 1. [1,2,5]Thiadiazolo[3,4-*c*][1,2,5]thiadiazole



model⁸ with contacts of like spin density of neighboring paramagnetic species in the solid state. At the same time, the presence of weak ferromagnetic (FM) interactions, most likely caused by contacts of unlike spin density in the heterospin salts, was also recognized.^{4–7}

Received: May 8, 2015

Published: June 29, 2015

The approach based on MAr_2 compounds may be generalized^{4c} since first ionization energies are practically equal for $\text{M} = \text{Cr}, \text{Mo},$ and W with the same Ar ligands.⁹ One may anticipate that heterospin RA salts with heavy atoms possessing strong spin–orbit coupling (SOC), Mo or W atoms, in the $[\text{MAr}_2]^+$ may satisfy the Dzyaloshinsky–Moriya mechanism for antisymmetric exchange leading to a spin canting even under conditions of AF exchange interactions between paramagnetic centers.^{4c,8c,10}

Very recently, for a weak organic ferromagnet based on a selenium–nitrogen π -heterocyclic neutral radical, i.e., the radical composed of light atoms, a large value of spin–orbit mediated anisotropic exchange terms was observed to highlight the importance of SOC for organic functional materials where this effect was *a priori* considered as less significant. For this reason, the design and synthesis of magnetic functional materials featuring SOC is an interesting challenge (ref 11 and references therein).

In this work we report on synthesis of the title salt (**2**) by interaction of compound **1** with MoMes_2 ($\text{Mes} = \text{mesitylene}/1,3,5\text{-trimethylbenzene}$) together with experimental and theoretical studies into its magnetic properties. Salt **2** is the first chalcogen–nitrogen π -heterocyclic RA salt containing an atom with non-negligible SOC in the cation.

EXPERIMENTAL AND COMPUTATIONAL DETAILS

General Procedure. All operations were carried out under argon using glovebox and Schlenk techniques. Solvents were dried by common methods and distilled under argon or by using an MBraun solvent drying system.

Compound **1** was synthesized and purified as described before.¹² Compounds MoMes_2 and MoTol_2 were prepared by literature methods¹³ and purified additionally by recrystallization and vacuum sublimation. The samples were diamagnetic in the solid state and solution according to EPR. MoMes_2 , found (calcd for $\text{C}_{18}\text{H}_{24}\text{Mo}$): C, 63.8 (64.3); H, 7.3 (7.2); Mo, 28.0 (28.5).

Elemental Analysis. Elemental analyses for C, H, N, and S were performed with an automatic Eurovector 600 analyzer. The samples were weighted and packed in the glovebox. For Mo, the weighed samples were dissolved in aqua regia, converted to alkaline solution with 10% ammonium hydroxide, and analyzed by means of Thermo Scientific iCAP 6500 spectrometer.

Crystallographic Analysis. Single-crystal X-ray diffraction data for **2** were collected at 150(2) K with the graphite-monochromatized Mo $K\alpha$ radiation ($\lambda = 0.71073 \text{ \AA}$) on a Bruker DUO APEX diffractometer equipped with a 4K CCD area detector. The φ -scan technique was employed to measure intensities. Absorption correction was applied using the SADABS program.¹⁴ The crystal structure of **2** was solved by direct methods and refined by the full-matrix least-squares techniques with the SHELXTL package.¹⁵ Atomic thermal parameters for non-hydrogen atoms were refined anisotropically. The hydrogen atoms of methyl groups were localized geometrically and refined using the riding model.

Crystallographic Data for Compound 2. $\text{C}_{20}\text{H}_{24}\text{MoN}_4\text{S}_2$, $M = 480.49$, triclinic, space group $P\bar{1}$, $a = 8.4459(3) \text{ \AA}$, $b = 8.4852(3) \text{ \AA}$, $c = 14.5051(6) \text{ \AA}$, $\alpha = 95.139(2)^\circ$, $\beta = 104.494(2)^\circ$, $\gamma = 92.145(2)^\circ$, $V = 1000.45(7) \text{ \AA}^3$, $T = 150 \text{ K}$, $Z = 2$, $\rho_{\text{calcd}} = 1.595 \text{ g cm}^{-3}$, $\mu(\text{Mo } K\alpha) = 0.877 \text{ mm}^{-1}$, crystal size $0.20 \times 0.15 \times 0.05 \text{ mm}^3$, reflections measured 7735 [3458 unique, 2832 with $I \geq 2\sigma(I)$], $R_{\text{int}} = 0.0488$, no. of params =

250, $R1 = 0.0352$ [for $I \geq 2\sigma(I)$], $wR2 = 0.0740$ [all reflections], $\Delta\rho_{\text{min,max}} = -0.595, 0.568 \text{ e \AA}^{-3}$, GOF = 0.981.

CCDC 1062310 contains the supplementary crystallographic data for this paper. The data can be obtained free of charge from the Cambridge Crystallographic Data Center via www.ccdc.cam.ac.uk/data_request/cif.

The XRD structure was used in quantum chemical modeling magnetic properties of salt **2**.

EPR Measurements. EPR spectra were obtained with two instruments: (1) The first is a Bruker ELEXSYS-II E500/540 spectrometer (X-band, microwave (MW) frequency $\sim 9.87 \text{ GHz}$, MW power of 20 mW, modulation frequency of 100 kHz, and modulation amplitude of 0.005 mT) equipped with a high-Q cylindrical resonator ER 4119HS. The g -values were measured with respect to 2,2-diphenyl-1-picrylhydrazyl (DPPH, $g = 2.0036$). Variable-temperature solution measurements were performed with a digital temperature control system ER 4131VT. (2) The second is a Bruker EMX 10/12 spectrometer (X-band, MW frequency $\sim 9.83 \text{ GHz}$, MW powers of 1–20 mW, modulation frequency of 100 kHz, and modulation amplitudes of 0.005–0.02 mT) equipped with a cylindrical resonator ER 4103TM.

Magnetic Measurements. The magnetic susceptibility measurements were performed with an MPMS-XL Quantum Design SQUID magnetometer in the temperature range 2–300 K in magnetic fields up to 5000 Oe. Linearity of magnetic field dependence of magnetization at 5 K (Supporting Information, Figure S1) evidenced the absence of FM impurities in the samples. For the calculation of the molar magnetic susceptibility (χ), the diamagnetic corrections were estimated using Pascal's constants.¹⁶ The effective magnetic moment (μ_{eff}) of salt **2** was calculated using the following equation: $\mu_{\text{eff}}(T) = [(3k/N_A\mu_B^2)\chi T]^{1/2} \approx (8\chi T)^{1/2}$.

Cyclic Voltammetry Measurements. The CV measurements on MoMes_2 and MoTol_2 (1.2 and 0.7 mM solutions in MeCN, respectively) were performed with a PG 310 USB potentiostat (HEKA Elektronik) at 293 K in an argon atmosphere at a stationary Pt cylindrical electrode ($S = 0.16 \text{ cm}^2$) with 0.1 M Et_4NClO_4 as a supporting electrolyte. The potential sweep rate was 0.1 V s^{-1} . A standard electrochemical cell of 5 mL solution volume connected to the potentiostat with a three-electrode scheme was used. Peak potentials were quoted with reference to a saturated calomel electrode (SCE). First oxidation peaks for both compounds were diffusion-controlled, i.e., $I_p^{\text{A}}\nu^{-1/2} = \text{const}$, where I_p^{A} is the peak current.

Quantum Chemical Calculations. Parameters of the Heisenberg spin-Hamiltonian ($\hat{H} = -2\sum_{ij} J_{ij}\vec{S}_i\vec{S}_j$), viz., the pair exchange coupling constants J_{ij} , were calculated quantum chemically. The spin-unrestricted broken-symmetry (BS) approach¹⁷ was employed for the calculations of exchange interactions between RAs $[\text{1}]^-$ and between cations $[\text{MoMes}_2]^+$. These calculations were performed by DFT methods with the UB3LYP functional¹⁸ and the def2-TZVP basis set with ECP for Mo¹⁹ using the ORCA program package.²⁰ The J values were calculated according to the following formula:

$$J = -\frac{(E^{\text{HS}} - E_{\text{BS}}^{\text{LS}})}{\langle S^2 \rangle^{\text{HS}} - \langle S^2 \rangle_{\text{BS}}^{\text{LS}}}$$

Here, E^{HS} is the energy of the high-spin state of the pair, and $E_{\text{BS}}^{\text{LS}}$ is the energy of the low-spin state.

The exchange interactions between $[1]^-$ and $[\text{MoMes}_2]^+$ were calculated at the CASSCF(6,6)/ANO-RSS level. The active space of the CASSCF calculations consisted of five d-AOs of Mo and the SOMO of RA $[1]^-$. In addition, the electronic structure and energies of a series of lowest states, as well as the ground state g-tensor, were calculated for $[\text{MoMes}_2]^+$ at the CASSCF(9,9) and CASSCF(9,9)/RASSI/SINGLE_ANISO²¹ levels with ANO-RCC basis set.²² The active space of these CASSCF calculations consisted of five d-AOs of Mo and two π -bonding and two π^* -antibonding MOs of Mes ligands. The MOLCAS 8.0 program package²³ was employed for the CASSCF calculations.

Synthesis of Salt 2. At $-50\text{ }^\circ\text{C}$, a solution of 0.039 g (0.271 mmol) of **1** in 10 mL of tetrahydrofuran (THF) was added slowly via Teflon capillary to a stirred solution of 0.095 g (0.282 mmol) of MoMes_2 in 10 mL of THF. The reaction mixture immediately turned crimson, and then precipitation of a solid began. The reaction mixture was warmed-up to ambient temperature, and the almost colorless solvent was decanted from the precipitate. The latter was washed with $2 \times 5\text{ mL}$ of Et_2O and dried under vacuum. Salt $[\text{MoMes}_2]^+[1]^-$ (**2**) was obtained in the form of microcrystalline brown solid, 0.111 g (83%). Found (calcd for $\text{C}_{20}\text{H}_{24}\text{MoN}_4\text{S}_2$): C, 49.0 (50.0); H, 5.0 (5.0); Mo, 19.4 (20.0); N, 11.7 (11.5); S, 13.1 (13.4).²⁴ For this product, solid-state EPR and magnetic measurements were performed. The product was dissolved in DMF to give a red solution for EPR measurements.

Orange plate-like single crystals of **2** suitable for XRD were obtained from the reaction between **1** and MoMes_2 (0.15 mmol each) in 3 mL of DMF performed at $-50\text{ }^\circ\text{C}$, followed by concentration of the reaction solution under vacuum at $-5\text{ }^\circ\text{C}$ to a half of the volume and storage overnight at $-24\text{ }^\circ\text{C}$.

During storage in a glovebox at ambient temperature, the product gradually released liquid (mesitylene, bp $165\text{ }^\circ\text{C}$) and changed its color to black in the course of 1 month, while in concentrated DMF solution, or in the solid state in contact with DMF/ether mixture, the compound turned black in 1–2 days depending on the concentration and temperature (in the case of solution, appearing as black precipitate).

The black product obtained after storing salt **2** at ambient temperature had lost ca. 30% of its weight (after evacuation) and solubility in DMF. According to the elemental analysis data, the black compound had formula $[\text{MoMes}_y][\text{C}_2\text{N}_4\text{S}_2]$, $y = 0.7\text{--}1$, featuring the spontaneous loss of the Mes ligands. According to solid-state EPR and magnetometry, the final decomposition product was diamagnetic, whereas the intermediates revealed paramagnetic properties different from those of initial salt **2** (see below).

RESULTS AND DISCUSSION

Quite unexpectedly, the redox properties of MoMes_2 and MoTol_2 were not quantitatively characterized to date. According to the cyclic voltammetry (CV) data, the first step of the electrochemical oxidation of both MoTol_2 ($E_p^{1A} = -0.71\text{ V}$) and MoMes_2 ($E_p^{1A} = -0.79\text{ V}$) in MeCN solutions is a one-electron reversible process ($I_p^C/I_p^{1A} \approx 1$, $E_p^{1A} - E_p^{1C} = 0.06\text{ V}$, $E_p^{1A} - E_p^{1A/2} = 0.06\text{ V}$) associated with the formation of the long-lived radical cation (Supporting Information, Figure S2, Table S1). The remarkably negative potential at which MoAr_2 (Ar = Tol, Mes) get oxidized is quantitative evidence for their description as *strong* electron donors comparable with the well-known tetrakis(dimethylamino)ethylene whose oxidation potential measured under similar conditions is -0.78 V .²⁵ The

equilibrium constant of the electron transfer from MoMes_2 onto **1** with formation of radical-ion salt $[\text{MoMes}_2]^+[1]^-$ (**2**) can be estimated from the standard equation $K = \exp[-F(E_{\text{MoMes}_2}^0 - E_1^0)/RT]$ with $E_{\text{MoMes}_2}^0 = -0.82\text{ V}$ and $E_1^0 = -0.56\text{ V}$ calculated from the CV data of MoMes_2 (this work) and **1** in MeCN. The values of $K = 7.55 \times 10^5$ at 223 K and 2.78×10^4 at 295 K are favorable for the radical-ion salt **2**.

With MoMes_2 , compound **1** was chemically reduced in THF into air-sensitive heterospin salt $[\text{MoMes}_2]^+[1]^-$ (**2**, Scheme 1) whose identity was confirmed by elemental analysis, single-crystal X-ray diffraction (XRD; Figure 1), solid-state and solution EPR (Figure 2), and magnetic measurements (Figure 3).

Scheme 1. Synthesis of Salt $[\text{MoMes}_2]^+[1]^-$ (**2**)

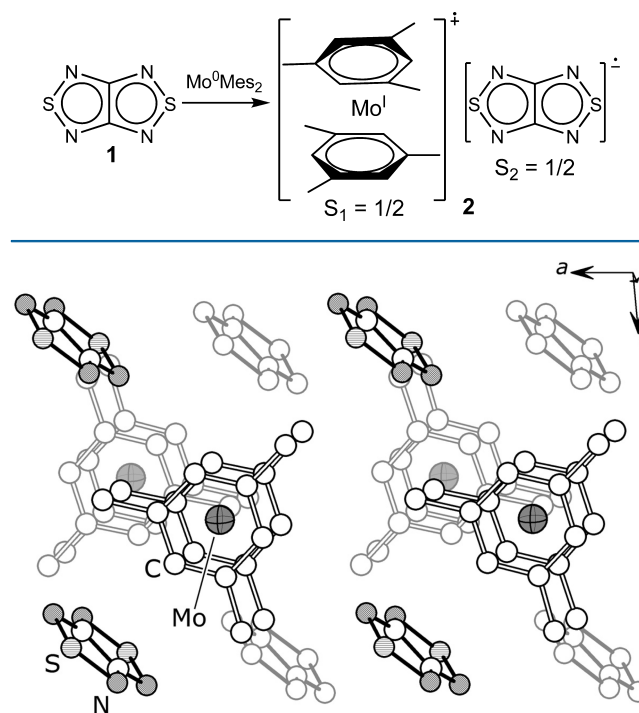


Figure 1. Crystal structure of salt **2** with layers of the anions and cations alternating across the b axis (H atoms are not shown, rear molecules are faded).

According to the XRD data, the structure of salt **2** is composed of cations $[\text{MoMes}_2]^+$ in the eclipsed conformation and flat RAs $[1]^-$, with both ions in common positions of the crystal lattice. The structure is composed of layers of cations and anions spreading in the (010) planes (Figure 1). The RAs are inclined by $\sim 44.7^\circ$ off the layer plane and aligned along the [101] direction. The distances between the S atoms of neighboring RAs are 3.45 and 3.89 Å; the former are slightly less than double the VdW radius of S (3.6 Å).²⁶ The cations lie nearly parallel to the layer plane considering the vector between ring centroids of two Mes ligands. One Me group of each Mes protrudes into the anionic layer; i.e., each RA is sufficiently encompassed by Me groups of adjacent cations. Such layered crystal packing of **2** is different from that of related radical-ion salt $[\text{CrTol}_2]^+[1]^-$ but similar to the packing of salt $[\text{CrTol}_2]^+[3]^-$ (**3** = [1,2,5]thiadiazolo[3,4- b]pyrazine).^{7a} The latter contains more flattened layers of the anions and more

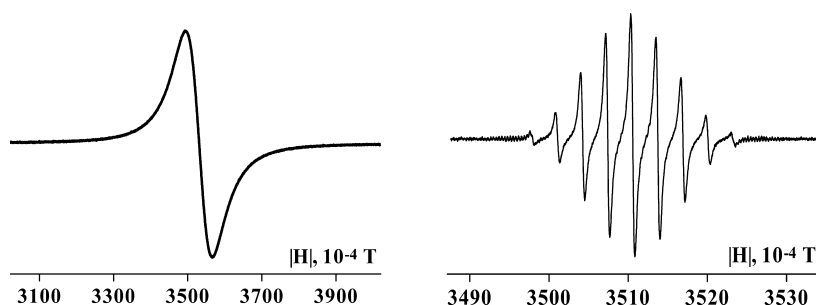


Figure 2. EPR spectra of salt **2** in the solid state (left) and in DMF solution (right). The solution spectrum is identical to that of the authentic RA $[1]^-$.²⁷

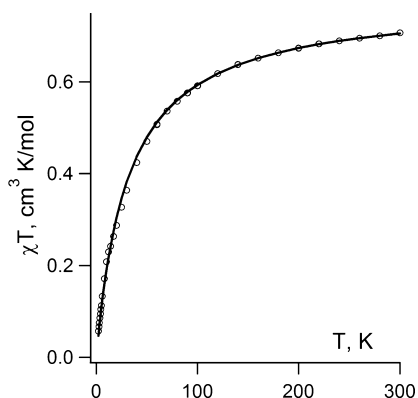


Figure 3. Experimental (O) temperature dependence of the molar magnetic susceptibility of salt **2**, $\chi(T)$, in the form of product χT in the temperature range 2–300 K together with its Curie–Weiss treatment (—).

loose layers of the cations which are apparently dependent on the steric demand of molecule **3**.

Whereas magnetic measurements confirmed that salt **2** is a heterospin, $S_1 = S_2 = 1/2$, system (see below), in a DMF solution of **2** only the RA $[1]^-$ ²⁷ was detected by EPR (Figure 2). This is reasonable since in contrast to the well-resolved solution EPR spectrum of $[\text{MoToI}_2]^+$ that of $[\text{MoMes}_2]^+$ in various solvents (e.g., MeCN, THF, EtOH) was reported as an unresolved broad signal centered at $g = 1.9857$ ¹³ (Supporting Information, Figures S3–S5). It should be noted that progressive loss of spectral resolution with increasing methyl substitution on the aromatic rings of related species $[\text{CrAr}_2]^+$ is known.¹³

Magnetic measurements on salt **2** revealed that at 300 K the product of temperature and molar magnetic susceptibility, χT , is equal to $0.71 \text{ cm}^3 \text{ K mol}^{-1}$ ($\mu_{\text{eff}} = 2.40 \mu_{\text{B}}$) which is close to the value $0.75 \text{ cm}^3 \text{ K mol}^{-1}$ ($\mu_{\text{eff}} = 2.45 \mu_{\text{B}}$) expected for system of two noncorrelated spins $S_1 = S_2 = 1/2$ with $g = 2$. On lowering the temperature, χT monotonically decreases. In the whole temperature range 2–300, molar magnetic susceptibility is well-described by Curie–Weiss law (Figure 3) with parameters C and θ equal to $0.78 \pm 0.01 \text{ cm}^3 \text{ K mol}^{-1}$ and $-31.2 \pm 0.2 \text{ K}$, respectively, implying the dominance of AF interactions. For salt **2**, θ is 4-fold bigger than $\theta = -7.1 \text{ K}$ for analogous salt $[\text{CrToI}_2]^+[1]^-$,^{7a} and this might be an indication of the SOC contribution to AF exchange coupling in **2**.

In the mean-field approximation, the value of θ is described by the following equation:

$$\theta = \frac{2S(S+1)}{3k} \sum_{m=1}^{N'} z_m J_m$$

Here z_m is the number of paramagnetic neighbors with spin S around every paramagnetic species coupled by the exchange interaction J_m .²⁸ Therefore, for salt **2** the exchange interactions between a selected paramagnetic species and its paramagnetic neighbors may be estimated in whole as $\sum_{m=1}^{N'} z_m J_m = -43.4 \text{ cm}^{-1}$. The negative θ and decrease of χT with lowering temperature imply the dominance of AF interactions between paramagnetic centers in solid **2**.

Overall, the experimental magnetic behavior of **2** is similar to that of salts $[\text{CrToI}_2]^+[1]^-$, $[\text{CrCp}^*_2]^+[1]^-$, and $[\text{CoCp}_2]^+[1]^-$,⁷ as well as the salt $[\text{CoCp}_2]_2[4]_3$ (**4** = naphtha[2,3-*c*][1,2,5]thiadiazole-4,9-dione).²⁹ Particularly, for salts $[\text{MAR}_2]^+[1]^-$ changing the cation 3d atom $M = \text{Cr}$ ($Z = 24$) with weak SOC by a 4d atom $M = \text{Mo}$ ($Z = 42$) with stronger SOC does not affect their macroscopic magnetic properties.

Quantum chemical calculations of the properties of the cation $[\text{MoMes}_2]^+$ and exchange interactions between paramagnetic centers of the salt **2** were performed at various levels of theory including DFT and CASSCF. The utility of DFT applications to transition metal derivatives has been comprehensively discussed recently.³⁰ First of all, properties of the cation $[\text{MoMes}_2]^+$ were calculated using CASSCF(9,9)/RASSI method, and 10 sextets, 20 quartets, and 20 doublets were taken into account in the calculations. The ground state of $[\text{MoMes}_2]^+$ was found to be a doublet, as well as the first and second excited states lying 9542 and 10 546 cm^{-1} higher in energy. The lowest quartet and sextet states were found to be 30 980 and 59 430 cm^{-1} above the ground state. Taking into account SOC, the components of the g -tensor were calculated for the ground Kramers doublet as $g_x = 2.007$, $g_y = 2.001$, $g_z = 1.966$, and $g_{\text{iso}} = 1.991$. Thus, the cation $[\text{MoMes}_2]^+$ in the ground state has almost, but not exactly, an isotropic g -tensor. On the contrary, the second doublet state has a very anisotropic g -tensor with $g_x = 1.686$, $g_y = 1.688$, $g_z = 3.836$, and $g_{\text{iso}} = 2.403$.

Earlier, we demonstrated that the pair exchange interactions between RAs $[1]^-$ in their salts with various cations,^{4b,c,5,7} as well as those between cations $[\text{CrR}_2]^+$ ($R = \text{Cp}^*$, Tol) in the corresponding heterospin salts,⁷ can be reproduced with good accuracy in the calculations using a spin-unrestricted BS approach at the UB3LYP level of theory. Unfortunately, we did not succeed in estimating correctly the exchange interactions between $[1]^-$ and $[\text{CrR}_2]^+$ using the BS approach, and the CASSCF or CASSCF/NEVPT2 methods were used to calculate these interactions.⁷ Therefore, the same approaches

were employed in this work to estimate pair exchange interactions between paramagnetic ions of salt **2**.

In the crystals of **2**, all RAs [1]⁻ are structurally equivalent. Every single RA has 10 nearest-neighboring RAs with shortest S...S distances ($R_{S...S}$) less than 10 Å. According to the UB3LYP/def2-TZVP calculations, only two exchange interactions with $R_{S...S}$ of ~3.45 and ~3.89 Å (Figure S6, Supporting Information) should be taken into account while exchange coupling with $R_{S...S} > 7.2$ Å can be neglected ($|J| < 0.1$ cm⁻¹). The J values for pairs with $R_{S...S} = 3.45$ and 3.89 Å were calculated as $J_1 = -12.9$ cm⁻¹ and $J_2 = 2.8$ cm⁻¹. One can conclude that the RA magnetic subsystem can be approximated by alternating chains of RAs (Figure S6, Supporting Information) coupled by both AF and FM interactions.

All cations [MoMes₂]⁺ are also structurally equivalent, and every single cation has 7 nearest-neighboring cations with the Mo...Mo ($R_{Mo...Mo}$) distances less than 10 Å (Figure S7, Supporting Information). According to the UB3LYP/def2-TZVP calculations with ECP for Mo, the J parameters for the cation pairs have both signs and are in the range $-0.72 < J < 0.22$ cm⁻¹. The largest absolute values of J were calculated for the pairs with $R_{Mo...Mo}$ of ~7.01 and ~7.95 Å as -0.72 and -0.48 cm⁻¹, respectively. The strongest FM interaction of 0.22 cm⁻¹ was calculated for the pair with $R_{Mo...Mo}$ of 8.44 Å (Figure S7, Supporting Information).

Besides, every single cation has four nearest-neighboring RAs connected to it by three magnetic couplings. The values of J parameters calculated at the CASSCF(6,6)/ANO-RCC level are -3.9 , 0.08 , and 0.06 cm⁻¹ for $R_{Mo...S} = 5.22$, 6.93 , and 5.90 Å, respectively (Figure S8, Supporting Information).

Thus, the magnetic structure of salt **2** is complex and characterized by a presence of both AF and FM interactions ranging from -12.9 to 2.7 cm⁻¹ with dominance of the AF interactions. Stronger exchange coupling between paramagnetic centers in salt **2** ($|J| \leq 13$ cm⁻¹) results in higher value of Weiss constant θ as compared with that of the analogous salt [CrToI₂]⁺[1]⁻.^{7a}

Upon storage at ambient temperature in a glovebox, salt **2** isolated from the reaction mixture as a brown solid soluble in DMF spontaneously changed its color into black, and the black substance was insoluble in DMF. This behavior is different from that of previously studied RA salts of compound **1** with cations [CrToI₂]⁺, [CrCp*₂]⁺, and [CoCp₂]⁺.^{6,7} Elemental analysis data indicated decomposition with partial loss of Mes ligands. According to solid-state EPR and magnetometry, the final decomposition product is diamagnetic, whereas partially decomposed samples revealed interesting paramagnetic properties different from those of initial salt **2** (Figure S9, Supporting Information) worthy of special study. Particularly, the effective magnetic moment of such samples decreases monotonically in temperature range 300–12 K but then increases sharply in the range 12–2 K.

Under the same reaction conditions as those for the synthesis of salt **2**, interaction of compound **1** with MoToI₂ gave an insoluble black product whose elemental analysis data implied partial loss of the Tol ligands.³¹ According to the magnetic measurements, the product is diamagnetic. It should be noted that redox reactions occurring with partial or total loss of Ar ligands are well-known for MAr₂ derivatives³² particularly for those of Mo and W.³³ Noticeably, loss of Cp* ligand was also observed in the reaction between [1,2,5]thiadiazolo[3,4-*b*]-quinoxaline (**5**) and CrCp*₂ where the only isolated product

was cubane cluster [Cp*CrS]₄ characterized by XRD (Figure S10, Supporting Information).³⁴

The loss of Ar ligand in the case of MoToI₂ and its absence in the case of MoMes₂ in the reactions with compound **1** is consistent with the generally observed increase in stability of the M–Ar bond upon increasing methyl substitution.³²

CONCLUSIONS

Molecular magnetic materials based on 4d and 5d transition metals attract much current attention due to stronger exchange interactions, higher magnetic anisotropy, and potential multifunctional properties.³⁵ Reaction between MoMes₂ and thiadiazole **1** gave an air-sensitive and thermally unstable heterospin ($S_1 = S_2 = 1/2$) radical-ion salt **2**. The structure of **2** was unambiguously confirmed by XRD in combination with EPR and magnetometry. The cation of **2** contains 4d atom Mo ($Z = 42$) with relatively strong SOC; however, no definite manifestation of the latter in macroscopic magnetic properties of **2** was observed. At the same time, the θ value for **2** is bigger than that for analogous salt [CrToI₂]⁺[1]⁻ ($-\theta = 31.2$ and 7.1 K, respectively) whereas the g -tensor of cation [MoMes₂]⁺ in the ground state is not *exactly* isotropic. These features might imply very small magnetoanisotropy due to SOC.

Quantum chemical calculations performed with the BS DFT and CASSCF approaches revealed complex 3D magnetic structure of salt **2** featuring both the FM and AF exchange interactions with the dominance of the latter.

Upon storage at ambient temperature, salt **2** slowly decomposes with partial loss of Mes ligands. The final decomposition product is diamagnetic.

Further work in the field may be focused on organometallics WAR₂ as reducing agents providing target radical-ion salts with stronger SOC in their cations (W , $Z = 74$). Enlarged SOC in the RAs can be associated with heavier chalcogens Se ($Z = 34$) and especially Te ($Z = 52$). The chemistry of 1,2,5-selenadiazoles is well-developed,³⁶ and emerging chemistry of 1,2,5-telluradiazoles is progressing.³⁷ In contrast to Se congeners, however, 1,2,5-telluradiazolidyl RAs are unknown despite neutral 1,2,5-telluradiazoles being involved as electron acceptors in various charge-transfer processes. This makes generation and identification of these RAs a goal in itself.

ASSOCIATED CONTENT

Supporting Information

CV data for MoToI₂ and MoMes₂, and XRD data for salt **2** (CCDC-1062310) and the cubane cluster [Cp*CrS]₄ (CCDC-1053125). Crystallographic data in CIF format. The Supporting Information is available free of charge on the ACS Publications website at DOI: 10.1021/acs.inorgchem.5b01033.

AUTHOR INFORMATION

Corresponding Authors

*E-mail: gritsan@kinetics.nsc.ru.

*E-mail: zibarev@nioch.nsc.ru.

Notes

The authors declare no competing financial interest.

ACKNOWLEDGMENTS

The authors are grateful to Prof. Leonid A. Shundrin for valuable discussions, and to the Presidium of the Russian Academy of Sciences (Project 8.14), the Royal Society (RS International Joint Project 2010/R3), the Leverhulme Trust

(Project IN-2012-094), the Siberian Branch of the Russian Academy of Sciences (Project 13), the Ministry of Education and Science of the Russian Federation (Project of Joint Laboratories of Siberian Branch of the Russian Academy of Sciences and National Research Universities), and the Russian Foundation for Basic Research (Projects 13-03-00072 and 15-03-03242) for financial support of various parts of this work. N.A.S. thanks the Council for Grants of the President of Russian Federation for postdoctoral scholarship (grant MK-4411.2015.3). B.E.B. is grateful for an EaStCHEM Hirst Academic Fellowship. A.V.Z. thanks the Foundation named after D. I. Mendeleev, Tomsk State University, for support of his work.

REFERENCES

- (1) (a) Miller, J. S. *J. Mater. Chem.* **2010**, *20*, 1846–1857. (b) Her, J. H.; Stephens, P. W.; Ribas-Arino, J.; Novoa, J. J.; Shum, W. W.; Miller, J. S. *Inorg. Chem.* **2009**, *48*, 3296–3307. (c) Miller, J. S. *Polyhedron* **2009**, *28*, 1596–1605. (d) Miller, J. S. *Dalton Trans.* **2006**, 2742–2749. (e) *Magnetism: Molecules to Materials*; Miller, J. S., Drillon, M., Eds.; Wiley-VCH: Weinheim, Germany, 2005. (f) Miller, J. S. *Adv. Mater.* **2002**, *14*, 1105–1110. (g) Miller, J. S. *Inorg. Chem.* **2002**, *39*, 4392–4408. (h) Miller, J. S.; Epstein, A. J. *Angew. Chem., Int. Ed.* **1994**, *33*, 385–415. (i) Miller, J. S.; Epstein, A. J.; Reiff, M. W. *Chem. Rev.* **1988**, *88*, 201–220.
- (2) (a) Caneschi, A.; Gatteschi, D.; Sessoli, R.; Rey, P. *Acc. Chem. Res.* **1989**, *22*, 392–398. (b) Lemaire, M. T. *Pure Appl. Chem.* **2004**, *76*, 277–293. (c) Tretyakov, E. V.; Ovcharenko, V. I. *Russ. Chem. Rev.* **2009**, *78*, 971–1012. (d) Train, C.; Norel, L.; Baumgarten, M. *Coord. Chem. Rev.* **2009**, *253*, 2342–2351. (e) Ovcharenko, V. I. In *Stable Radicals: Fundamentals and Applied Aspects of Odd-Electron Compounds*; Hicks, R. G., Ed.; Wiley: New York, 2010. (f) Lemaire, M. T. *Pure Appl. Chem.* **2011**, *83*, 141–149. (g) Ratera, I.; Veciana, J. *Chem. Soc. Rev.* **2012**, *41*, 303–349. (h) Datta, S. N.; Trindle, C. O.; Illas, F. *Theoretical and Computational Aspects of Magnetic Organic Molecules*; Imperial College Press: London, U.K., 2013.
- (3) (a) Preuss, K. E. *Coord. Chem. Rev.* **2015**, *289–290*, 49–61. (b) Preuss, K. E. *Dalton Trans.* **2007**, 2357–2369.
- (4) (a) Lonchakov, A. V.; Rakitin, O. A.; Gritsan, N. P.; Zibarev, A. V. *Molecules* **2013**, *18*, 9850–9900. (b) Gritsan, N. P.; Zibarev, A. V. *Russ. Chem. Bull.* **2011**, *60*, 2131–2140. (c) Zibarev, A. V.; Mews, R. In *Selenium and Tellurium Chemistry: From Small Molecules to Biomolecules and Materials*; Woollins, J. D., Laitinen, R. S., Eds.; Springer: Berlin, 2011.
- (5) Makarov, A. Yu.; Chulanova, E. A.; Pushkarevsky, N. A.; Semenov, N. A.; Lonchakov, A. V.; Bogomyakov, A. S.; Irtegov, I. G.; Vasilieva, N. V.; Lork, E.; Gritsan, N. P.; Konchenko, S. N.; Ovcharenko, V. I.; Zibarev, A. V. *Polyhedron* **2014**, *72*, 43–49.
- (6) Konchenko, S. N.; Gritsan, N. P.; Lonchakov, A. V.; Irtegov, I. G.; Mews, R.; Ovcharenko, V. I.; Radius, U.; Zibarev, A. V. *Eur. J. Inorg. Chem.* **2008**, *2008*, 3833–3838.
- (7) (a) Semenov, N. A.; Pushkarevsky, N. A.; Suturina, E. A.; Chulanova, E. A.; Kuratieva, N. V.; Bogomyakov, A. S.; Irtegov, I. G.; Vasilieva, N. V.; Konstantinova, L. S.; Gritsan, N. P.; Rakitin, O. A.; Ovcharenko, V. I.; Konchenko, S. N.; Zibarev, A. V. *Inorg. Chem.* **2013**, *52*, 6654–6663. (b) Semenov, N. A.; Pushkarevsky, N. A.; Lonchakov, A. V.; Bogomyakov, A. S.; Pritchina, E. A.; Suturina, E. A.; Gritsan, N. P.; Konchenko, S. N.; Mews, R.; Ovcharenko, V. I.; Zibarev, A. V. *Inorg. Chem.* **2010**, *49*, 7558–7564.
- (8) (a) Fatila, E. M.; Clerac, R.; Jennings, M.; Preuss, K. E. *Chem. Commun.* **2013**, *49*, 9434–9433. (b) Hirel, C.; Luneau, D.; Pecaut, J.; Öhrström, L.; Bussiere, G.; Reber, C. *Chem.—Eur. J.* **2002**, *8*, 3157–3161. (c) Novoa, J. J.; Deumal, M. *Struct. Bonding (Berlin)* **2001**, *100*, 33–60. (d) Kahn, O. *Molecular Magnetism*; VCH Publishers: New York, 1993. (e) McConnell, H. M. *J. Chem. Phys.* **1963**, *39*, 1910–1917.
- (9) (a) Green, J. C. *Struct. Bonding (Berlin)* **1981**, *43*, 37–112. (b) Cloke, F. G. N.; Green, M. L. H.; Morris, G. E. *J. Chem. Soc., Chem. Commun.* **1978**, 72–74. (c) Evans, S.; Green, J. C.; Jackson, S. E. *J. Chem. Soc., Faraday Trans. 2* **1972**, *68*, 249–258. (d) Herberich, G. E.; Mueller, J. J. *Organomet. Chem.* **1969**, *16*, 11–117.
- (10) The strength of the SOC increases sharply with the atomic number Z as Z^4 to be sufficient for atoms with $Z > 30$ (for $M = \text{Cr}$, Mo , and W ; $Z = 24$, 42 , and 74 , respectively) or, in slightly different formulation, for atoms with principle quantum number $n \geq 5$.
- (11) (a) Thirunavukkuarasu, K.; Winter, S. M.; Beedle, C. C.; Kovalev, A. E.; Oakley, R. T.; Hill, S. *Phys. Rev. B* **2015**, *91*, 014412. (b) Winter, S. M.; Hill, S.; Oakley, R. T. *J. Am. Chem. Soc.* **2015**, *137*, 3720–3730. (c) Winter, S. M.; Oakley, R. T.; Kovalev, A. E.; Hill, S. *Phys. Rev. B* **2012**, *85*, 094430. (d) Winter, S. M.; Datta, S.; Hill, S.; Oakley, R. T. *J. Am. Chem. Soc.* **2011**, *133*, 8126–8129. (e) Mito, M.; Komorida, Y.; Tsuruda, H.; Tse, J. S.; Desgreniers, S.; Ohishi, Y.; Leitch, A. A.; Cvrkalj, K.; Robertson, C. M.; Oakley, R. T. *J. Am. Chem. Soc.* **2009**, *131*, 16012–16013. (f) Leitch, A. A.; Brusso, J. L.; Cvrkalj, K.; Reed, R. W.; Robertson, C. M.; Dube, P. A.; Oakley, R. T. *Chem. Commun.* **2007**, 3368–3370.
- (12) Pushkarevsky, N. A.; Lonchakov, A. V.; Semenov, N. A.; Lork, E.; Buravov, L. I.; Konstantinova, L. S.; Silber, T. G.; Robertson, N.; Gritsan, N. P.; Rakitin, O. A.; Woollins, J. D.; Yagubskii, E. B.; Beckmann, J.; Zibarev, A. V. *Synth. Met.* **2012**, *162*, 2267–2276. (b) Konstantinova, L. S.; Knyazeva, E. A.; Obruchnikova, N. V.; Gatilov, Yu. V.; Zibarev, A. V.; Rakitin, O. A. *Tetrahedron Lett.* **2013**, *54*, 3075–3078.
- (13) (a) Calucci, L.; Cloke, F. G. N.; Englert, U.; Hitchcock, P. B.; Pampaloni, G.; Pinzino, C.; Puccini, F.; Volpe, M. *Dalton Trans.* **2006**, 4228–4234. (b) Experimental hfc constants of $[\text{MoToL}]^+$ in DMF solution (mT): 0.483 (a_{ToL} ; 10H, carbocycle), 0.037 (a_{ToL} ; 6H, Me substituents), 1.465 (a_{Mo}), 1.506 (a_{ToL}). Chulanova, E. A. Diploma Work, Novosibirsk State University, Novosibirsk, Russia, 2014.
- (14) (a) APEX2 (version 2.0) and SAINT (version 8.18c); Bruker AXS Inc.: Madison, WI, 2000–2012. (b) SADABS (version 2.11); Bruker Advanced X-ray Solutions: Madison, WI.
- (15) Sheldrick, G. M. *Acta Crystallogr., Sect. A* **2008**, *64*, 112–122.
- (16) Kalinnikov, V. T.; Rakitin, Yu. V. *Introduction in Magnetochemistry. Method of Static Magnetic Susceptibility*; Nauka: Moscow, 1980; p 302 (in Russian).
- (17) (a) Nagao, H.; Nishino, M.; Shigeta, Y.; Soda, T.; Kitagawa, Y.; Onishi, T.; Yoshika, Y.; Yamaguchi, K. *Coord. Chem. Rev.* **2000**, *198*, 265–295. (b) Noodleman, L.; Case, D. A.; Mouesca, J. M. *Coord. Chem. Rev.* **1995**, *144*, 199–244. (c) Noodleman, L.; Davidson, E. R. *Chem. Phys.* **1986**, *109*, 131–143. (d) Noodleman, L. *J. Chem. Phys.* **1981**, *74*, 5737–5743.
- (18) (a) Becke, A. D. *J. Chem. Phys.* **1993**, *98*, 5648–5652. (b) Lee, C.; Yang, W.; Parr, R. G. *Phys. Rev. B* **1988**, *37*, 785–789.
- (19) (a) Weigend, F.; Ahlrichs, R. *Phys. Chem. Chem. Phys.* **2005**, *7*, 3297–3305. (b) Schaefer, A.; Horn, H.; Ahlrichs, R. *J. Chem. Phys.* **1992**, *97*, 2571–2577.
- (20) (a) Neese, F. *WIREs Comput. Mol. Sci.* **2012**, *2*, 73–78. (b) Neese, F.; Becker, U.; Ganyushin, G.; Hansen, A.; Izsak, R.; Liakos, D. G.; Kollmar, C.; Kossmann, S.; Pantazis, D. A.; Petrenko, T.; Reimann, C.; Riplinger, C.; Roemelt, M.; Sandhöfer, B.; Schapiro, I.; Sivalingam, K.; Wennmohs, F.; Weizsl, B.; Kállay, M.; Grimme, S.; Valeev, E. ORCA—An ab Initio, DFT and Semiempirical SCF-MO Package, Version 3.0; Max Planck Institute for Chemical Energy Conversion: Mülheim an der Ruhr, Germany.
- (21) (a) Chibotaru, L. F.; Ungur, L. *J. Chem. Phys.* **2012**, *137*, 064112. (b) Roos, B. O.; Malmqvist, P.-A. *Phys. Chem. Chem. Phys.* **2004**, *6*, 2919–2927. (c) Malmqvist, P.-A.; Roos, B. O.; Schimmelpfennig, B. *Chem. Phys. Lett.* **2002**, *357*, 230–240.
- (22) (a) Roos, O.; Lindh, R.; Malmqvist, P.-A.; Veryazov, V.; Widmark, P.-O. *J. Phys. Chem. A* **2005**, *109*, 6575–6579. (b) Roos, B. O.; Lindh, R.; Malmqvist, P.-A.; Veryazov, V.; Widmark, P.-O. *Chem. Phys. Lett.* **2005**, *409*, 295–299.
- (23) Aquilante, F.; De Vico, L.; Ferre, N.; Ghigo, G.; Malmqvist, P.-A.; Neogrady, P.; Pedersen, T. B.; Pitoňák, M.; Reiher, M.; Roos, B.

O.; Serrano-Andres, L.; Urban, M.; Veryazov, V.; Lindh, R. J. *Comput. Chem.* **2010**, *31*, 224–247.

(24) The sum of experimental percentages of C, H, Mo, N, and S in **2** is 98.2%, and besides H, all experimental values are somewhat lower than theoretical ones, especially for C. It can be explained by partial formation of molybdenum carbide (nitride and sulfide, respectively) during high-temperature decomposition of **2** in the analytical procedures employed. Importantly, the analysis of carefully purified starting MoMes₂ has shown the similar trend (see General Procedure in Experimental and Computational Details). In any case, formation of molybdenum carbides by high-temperature decomposition of various Mo/C compounds is well-known; see, for example: Wan, C.; Regmi, Y. N.; Leonard, B. M. *Angew. Chem., Int. Ed.* **2014**, *53*, 6407–6410.

(25) (a) Garnier, J.; Kennedy, A. R.; Berlouis, L. E. A.; Murphy, J. A.; Turner, A. T. *Beilstein J. Org. Chem.* **2010**, *6*, article 73. (b) Bock, H.; Ruppert, K.; Naether, C.; Havlas, Z.; Herrmann, C.; Arad, H. F.; Goebel, I.; John, A.; Meuret, J.; Nick, S.; Rauschenbach, A.; Seitz, W.; Vaupel, T.; Solouki, B. *Angew. Chem., Int. Ed.* **1992**, *31*, 550–581. (c) Wiberg, N.; Buchler, J. W. *Chem. Ber.* **1963**, *96*, 3223–3229.

(26) Mantina, M.; Chamberlin, A. C.; Valero, R.; Cramer, C. J.; Truhlar, D. G. *J. Phys. Chem. A* **2009**, *113*, 5806–5812.

(27) (a) Makarov, A. Yu.; Irtegov, I. G.; Vasilieva, N. V.; Bagryanskaya, I. Yu.; Borrmann, T.; Gatilov, Yu. V.; Lork, E.; Mews, R.; Stohrer, W. D.; Zibarev, A. V. *Inorg. Chem.* **2005**, *44*, 7194–7199. (b) Ikorskii, V. N.; Irtegov, I. G.; Lork, E.; Makarov, A. Yu.; Mews, R.; Ovcharenko, V. I.; Zibarev, A. V. *Eur. J. Inorg. Chem.* **2006**, *2006*, 3061–3067.

(28) (a) O'Connor, C. J. *Prog. Inorg. Chem.* **1982**, *29*, 203–283. (b) Myers, B. E.; Berger, L.; Friedberg, S. J. *Appl. Phys.* **1969**, *40*, 1149–1151.

(29) Morgan, I. S.; Jennings, M.; Vindigni, A.; Clerac, R.; Preuss, K. *Cryst. Growth Des.* **2011**, *11*, 2520–2527.

(30) Cramer, C. J.; Truhlar, D. G. *Phys. Chem. Chem. Phys.* **2009**, *11*, 10757–10816.

(31) Interactions of three other fused 1,2,5-thiadiazoles, namely, **3**, **5**, and bis([1,2,5]thiadiazolo)-[3,4-*b*;3',4'-*e*]pyrazine (**6**), with MoMes₂ and MoTol₂ were also studied. With MoTol₂, reactions featured partial loss of the Tol ligands and gave insoluble diamagnetic products. With MoMes₂, experiments are still in progress; however, it should be mentioned that in the case of **6** DMF-soluble brown product was obtained and determined to be paramagnetic in the solid state and solution. The results will be published elsewhere.

(32) (a) Pampaloni, G. *Coord. Chem. Rev.* **2010**, *254*, 402–419. (b) Morris, M. J. In *Comprehensive Organometallic Chemistry II*; Abel, E. W., Stone, F. G. A., Wilkinson, G., Eds.; Pergamon: Oxford, U.K., 1995; Vol. 5, Vanadium and Chromium Groups; Chapter 8, Arene and Heteroarene Complexes of Chromium, Molybdenum and Tungsten, pp 471–549.

(33) (a) Bandy, J. A.; Mtetwa, V. S. B.; Prout, K.; Green, J. C.; Davies, C. E.; Green, M. L. H.; Hazel, N. J.; Izquierdo, A.; Martin-Polo, J. J. *J. Chem. Soc., Dalton Trans.* **1985**, 2037–2049. (b) Brown, P. R.; Cloke, F. G. N.; Green, M. L. H.; Hazel, N. J. *J. Chem. Soc., Dalton Trans.* **1983**, 1075–1079. (c) Green, M. L. H.; Silverthorn, W. E. *J. Chem. Soc., Dalton Trans.* **1973**, 301–306.

(34) Pushkarevsky, N. A.; Naumov, D. Yu.; Konstantinova, L. S.; Rakitin, O. A.; Konchenko, S. N.; Zibarev, A. V. *Unpublished result*, 2010.

(35) Wang, X.-Y.; Avendano, C.; Dunbar, K. R. *Chem. Soc. Rev.* **2011**, *40*, 3213–3238.

(36) (a) Konstantinova, L. S.; Knyazeva, E. A.; Nefyodov, A. A.; Camacho, P. S.; Ashbrook, S. E. M.; Woollins, J. D.; Zibarev, A. V.; Rakitin, O. A. *Tetrahedron Lett.* **2015**, *56*, 1107–1110. (b) Konstantinova, L. S.; Knyazeva, E. A.; Rakitin, O. A. *Org. Prep. Proc. Int.* **2014**, *46*, 475–544. (c) Makarov, A. G.; Selikhova, N. Yu.; Makarov, A. Yu.; Malkov, V. S.; Bagryanskaya, I. Yu.; Gatilov, Yu. V.; Knyazev, A. S.; Slizhov, Yu. G.; Zibarev, A. V. *J. Fluorine Chem.* **2014**, *165*, 123–131. (d) Todress, Z. V. *Chalcogenadiazoles: Chemistry and Applications*; CCR Press/Taylor & Francis: London, U.K., 2012. (e) Vasilieva, N. V.; Irtegov, I. G.; Gritsan, N. P.; Lonchakov, A. V.; Makarov, A. Yu.

Shundrin, L. A.; Zibarev, A. V. *J. Phys. Org. Chem.* **2010**, *23*, 536–543. (f) Yamazaki, S. *Comprehensive Heterocyclic Chemistry III*; Katritzky, A. R., Ramsden, C. A., Scriven, E. F. V., Taylor, R. J. K., Eds.; Elsevier: Oxford, 2008; Vol. 6, pp 518–580. (g) Aitken, R. A. *Science of Synthesis*; Storr, R. C., Gilchrist, T. L., Eds.; Thieme: Stuttgart, 2003; Vol. 13, pp 777–822.

(37) (a) Garrett, G. E.; Gibson, G. L.; Straus, R. N.; Seferos, D. S.; Taylor, M. S. *J. Am. Chem. Soc.* **2015**, *137*, 4126–4133. (b) Semenov, N. A.; Lonchakov, A. V.; Gritsan, N. P.; Zibarev, A. V. *Izv. Akad. Nauk., Ser. Khim.* **2015**, 499–509. (c) Svec, J.; Zimcik, P.; Novakova, L.; Rakitin, O. A.; Amelichev, S. A.; Stuzhin, P. A.; Novakova, V. *Eur. J. Org. Chem.* **2015**, *2015*, 596–604. (d) Semenov, N. A.; Lonchakov, A. V.; Pushkarevsky, N. A.; Suturina, E. A.; Korolev, V. V.; Lork, E.; Vasiliev, V. G.; Konchenko, S. N.; Beckmann, J.; Gritsan, N. P.; Zibarev, A. V. *Organometallics* **2014**, *33*, 4302–4314. (e) Semenov, N. A.; Pushkarevsky, N. A.; Beckmann, J.; Finke, P.; Lork, E.; Mews, R.; Bagryanskaya, I.; Yu; Gatilov, Yu. V.; Konchenko, S. N.; Vasiliev, V. G.; Zibarev, A. V. *Eur. J. Inorg. Chem.* **2012**, *2012*, 3693–3703. (f) Cozzolino, A. F.; Elder, P. J. W.; Vargas-Baca, I. *Coord. Chem. Rev.* **2011**, *255*, 1426–1438. (g) Kovtonyuk, V. N.; Makarov, A. Yu.; Shakirov, M. M.; Zibarev, A. V. *Chem. Commun.* **1996**, 1991–1992. (h) Chivers, T.; Gao, X.; Parvez, T. *Inorg. Chem.* **1996**, *35*, 9–15. (i) Neidlein, R.; Knecht, D.; Gieren, A.; Ruiz-Perez, C. Z. *Naturforsch., B: J. Chem. Sci.* **1987**, *42*, 84–90. (j) Bertini, V.; Lucchesini, F.; De Munno, A. *Synthesis* **1982**, 681–683.